THE JOURNAL OF BIOLOGICAL CHEMISTRY VOL. 284, NO. 38, pp. 25791–25803, September 18, 2009

Rhythmic Expression of MicroRNA-26a Regulates the L-type Voltage-gated Calcium Channel α1C Subunit in Chicken Cone Photoreceptors*

Received for publication, June 15, 2009, and in revised form, July 14, 2009 Published, JBC Papers in Press, July 16, 2009, DOI 10.1074/jbc.M109.033993

Liheng Shi, Michael L. Ko, and Gladys Y.-P. Ko[1]

From the Department of Veterinary Integrative Biosciences, College of Veterinary Medicine and Biomedical Sciences, Texas A&M University, College Station, Texas 77843-4458

MicroRNAs (miRNAs) modulate gene expression by degrading or inhibiting translation of messenger RNAs (mRNAs). Here, we demonstrated that chicken microRNA-26a (gga-mir-26a) is a key posttranscriptional regulator of photoreceptor L-type voltage-gated calcium channel α1C subunit (L-VGCCα1C) expression, and its own expression has a diurnal rhythm, thereby explaining the rhythmic nature of L-VGCCα1Cs. Circadian oscillators in retinal photoreceptors provide a mechanism that allows photoreceptors to anticipate daily illumination changes. In photoreceptors, L-VGCC activities are under circadian control, which are higher at night and lower during the day. Interestingly, the mRNA level of VGCCα1D oscillates, but those for VGCCα1C do not. However, the protein expression of both VGCCα1C and α1D are higher at night in cone photoreceptors. The underlying mechanism regulating L-VGCCα1C protein expression was not clear until now. *In vitro* targeting reporter assays verified that gga-mir-26a specifically targeted the L-VGCCα1C 3′-untranslated region, and gga-mir-26a expression in the retina peaked during the day. After transfection with gga-mir-26a, L-VGCCα1C protein expression and L-VGCC current density decreased. Therefore, the rhythmic expression of gga-mir-26a regulated the protein expression of the L-VGCCα1C subunit. Additionally, both CLOCK (circadian locomoter output cycles kaput) and CREB (cAMP-response element-binding protein-1) activated gga-mir-26a expression *in vitro*. This result implies that gga-mir-26a might be a downstream target of circadian oscillators. Our work has uncovered new functional roles for miRNAs in the regulation of circadian rhythms in cone photoreceptors. Circadian regulated miRNAs could serve as the link between the core oscillator and output signaling that further govern biological functions.

MicroRNAs (miRNAs)[2] are a group of short, non-coding, single-stranded RNAs ~23 nucleotides in size, and they are regulatory elements targeting one or more downstream messenger RNAs (mRNAs), causing posttranscriptional degradation or translational repression (1–3). The mature miRNA is derived from a precursor sequence, which is transcribed from the genome by either RNA polymerase II or III, and miRNA expression shows tissue and developmental stage-specific patterns (1). Recently, several miRNAs have been reported to be involved in circadian rhythm (2–5). MicroRNA-219 and mir-132 influence the core oscillator in the mouse suprachiasmatic nucleus (SCN), the master clock. *In vivo* knockdown of mir-219 lengthens the circadian period, and mir-132 modulates light-induced clock resetting in mice (6). In the mouse retina, several miRNAs with high expression levels have been reported to be under circadian control. MicroRNA-182, mir-183, and mir-96 form a cluster in mouse chromosome 7, and they are highly expressed in the photoreceptor layer (7). Other miRNAs, such as mir-181a, mir-125b, mir-26a, mir-124a, mir-204, and mir-30c are expressed in different retina neurons, including photoreceptors (5, 7, 8). Whereas the mir-182/183/96 cluster and mir-124a are highly expressed at night, the mir-26a and mir-204 rhythm is anti-phase (5). Taken together, miRNAs play critical roles in both circadian input entrainment and output pathway in the SCN or retina.

The intrinsic circadian clocks govern various physiological functions and behaviors in animals, ranging from sleep and wakefulness to oscillations of body temperature, heart rate, hormone secretion, food intake, and locomotor activity to list a few (9–13). In the retina, circadian oscillators provide a mechanism for visual systems to initiate more sustained adaptive changes throughout the course of a day (13). The retina photoreceptor, a nonspiking sensory neuron, exerts its endogenous independent circadian oscillator to regulate physiological functions in anticipation of daily changes in ambient illumination (14, 15). The circadian regulation of photoreceptors includes outer segment disc shedding and renewal, retinomotor movement, morphological changes at synaptic ribbons, neurotransmitter release, and ion channel activity (16–22). Interlocking transcription/translation feedback loops, which in turn control signal transduction pathways, comprise the molecular mechanism underlying the circadian regulation of photoreceptors (13, 23). We previously brought to light how two ion channels are

* This work was supported, in whole or in part, by National Institutes of Health Grant RO1EY017452 (to G. K.). This work was also supported by a Department of Veterinary Integrative Bioscience programmatic development minigrant (to G. K.).

[1] To whom correspondence should be addressed: Dept. of Veterinary Integrative Biosciences, College of Veterinary Medicine and Biomedical Sciences, Texas A&M University, 4458 TAMU, College Station, TX 77843-4458. Tel.: 979-845-2828; Fax: 979-847-8981; E-mail: gko@cvm.tamu.edu.

[2] The abbreviations used are: miRNA, microRNA; SCN, suprachiasmatic nucleus; CNGC, cGMP-gated cation channel; L-VGCC, L-type voltage-gated calcium channel; ERK, extracellular signal-regulated kinase; Q-PCR, quantitative real time PCR; RT-PCR, reverse transcription-PCR; LD, light-dark; DD, dark-dark; ZT, Zeitgeber time; TK, thymidine kinase; Luc, luciferase; WT, wild type; eGFP, enhanced green fluorescent protein; pF, picofarads; CREB, cAMP-response element-binding protein; ANOVA, analysis of variance; E*n*, embryonic day *n*.

regulated by the circadian oscillators in chicken cone photoreceptors (18, 19, 24–26). The cGMP-gated cation channels (CNGCs) and L-type voltage-gated calcium channels (L-VGCCs) are both more active during the subjective night; however, the means by which the circadian oscillators control them are different. For CNGCs (18, 24), the apparent affinity for cGMP, the activating ligand, is higher during the subjective night than the subjective day, in which the ERK-mitogen-activated protein kinase signaling pathway plays a key role (18, 25). Maximum CNGC current is constant throughout the day, implying channel density remains constant. For L-VGCCs, current amplitudes are higher at night, and indeed channel expression in the cell membrane is higher at this time (19, 26). As with CNGCs, the ERK pathway plays a key role in the circadian regulation of L-VGCCs. However, in addition, the phosphatidylinositol 3-kinase-Akt pathway plays an equally important role in the circadian modulation of L-VGCCs (26).

The L-type VGCC is composed of four polypeptide subunits (α1(c, d, f), $\alpha 2\delta 1$, β, and γ), and the channel opens upon membrane depolarization, which allows calcium to enter neurons or muscle cells (27). The L-VGCCα1 subunits contain four transmembrane motifs and a long C-terminal regulatory domain, through which channel gating properties can be regulated by direct binding of calmodulin, phosphorylation, and other modifications (28–30). In chicken photoreceptors, the protein expression of the L-VGCCα1D subunit is higher during the subjective night with its mRNA levels peaking a few hours ahead (19). Although the mRNA levels of L-VGCCα1C, as detected by quantitative real time polymerase chain reaction (Q-PCR), do not change significantly throughout the day, the distribution of the L-VGCCα1C subunit in the cell membrane of cone photoreceptors shows a circadian rhythm (19). Thus, the mechanism underlying the circadian regulation of L-VGCCα1C in photoreceptors was not clear. To address this question, we investigated whether there were posttranscriptional regulation mechanisms that could affect L-VGCCα1C protein expression.

In our study detailed below, we showed that in the chicken retina, chicken mir-26a (gga-mir-26a) specifically targeted the L-VGCCα1C 3′-untranslated region (UTR) and inhibited L-VGCC channel activities in cone photoreceptors. The expression of gga-mir-26a was under circadian control, with levels higher during the day. As a result, gga-mir-26a modulated the protein expression of L-VGCCα1C in a circadian manner. Interestingly, both CLOCK (circadian locomoter output cycles kaput) and cAMP-response element-binding protein (CREB) were able to induce gga-mir26a expression *in vitro*. Hence, the circadian regulation of L-VGCCα1C subunit expression was through gga-mir-26a in the chicken retina.

EXPERIMENTAL PROCEDURES

Circadian Entrainment—Fertilized eggs (*Gallus gallus*) were obtained from the Poultry Science Department, Texas A&M University (College Station, TX). Chicken embryos from embryonic day 11 (E11) were entrained to 12:12 h light-dark (LD) cycles at 39 °C *in ovo*. Zeitgeber time 0 (ZT 0) was designated as the time when the lights came on, and ZT 12 was the time when the lights went off. After LD entrainment for 6 days *in ovo*, retinas were dissected out for biochemistry or molecular biology analysis at various Zeitgeber times of the day.

Plasmids—Chicken genomic DNA was prepared from the retina by homogenization in 500 mM Tris, pH 8.0, 20 mM EDTA, 10 mM NaCl, 1% SDS, and 500 μg/ml proteinase K. Protein digestion was carried out at 50 °C overnight. The DNA was extracted by phenol/chloroform and precipitated by 70% ethanol (31). The genomic DNA was used for PCR amplification of the gga-mir-26a and gga-mir-124a precursor sequences, the L-VGCCα1C 3′-UTR fragment, and the gga-mir-26a promoter. All PCR products were purified by a gel extraction kit (Qiagen, Valencia, CA) and cloned into pGEM Teasy (gga-mir-26a precursor and gga-mir-26a promoter; Promega, Madison, WI) or pBluescript II (L-VGCCα1C 3′-UTR; Stratagene, La Jolla, Ca) cloning vectors for sequence analysis. The gga-mir-26a precursor sequence was later ligated into a small RNA expression vector pSilencer 2.1-U6 neo (Applied Biosystems, Foster City, CA), whereas the gga-mir-26a promoter was ligated into a pGL3b vector (Promega, Madison, WI). The point mutation for the L-VGCCα1C 3′-UTR was prepared using the QuikChange® II site-directed mutagenesis kit (Stratagene, La Jolla, CA). The multimer 3′-UTR fragment was constructed by repeated ligation of the same fragment into the SpeI/XbaI site of a pBSII vector. The final four repeat fragment was cut out and ligated into pGL3-TK-Luc (XbaI; Promega). The 2-kb gga-mir-26a promoter region, the −150 to +1 promoter fragment (Δ-2kb−150), and the −2kb−300 promoter fragment (Δ−300-+1) were amplified by PCR and cloned into pGL3b. The E box region-specific deletion mutation of the gga-mir-26a promoter was constructed by direct ligation of the −150–+1 and −2kb−300 promoter fragments into pGL3b (SacI/NheI/XhoI). Mouse Clock (MGC-190424) and CREB (MGC-14010) clones were purchased from Invitrogen and constructed into each expression vector. All primers for this section are listed in Table 1.

Luciferase Reporter Assay—The COS1 cells were maintained in Dulbecco's modified Eagle's medium with 10% fetal bovine serum. Transfections were carried out using the TransIT®-COS transfection kit (Mirus, Madison, WI). For miRNA targeting assays, cells were cultured in 24-well plates and transfected with control or gga-mir-26a expression vector in combination with a reporter construct, TK-Luc4XWT (wild type) or TK-luc4Xmt (mutated) (150 ng each). TK-Luc4XWT contains a thymidine kinase (TK) minimum promoter that triggers luciferase (Luc) expression. Four copies of the control wild type (WT) gga-mir-26a target region from the chicken L-VGCCα1C 3′-UTR were inserted between the Luc coding sequence and SV40 poly(A) tail. TK-Luc4Xmt was similarly constructed except that it contained four repeats of a point-mutated mir-26a target sequence. The luciferase reporter assays (Promega) were performed 48 h after transfection, and relative luciferase activity was determined by luminosity (PerkinElmer Life Sciences). All luciferase activities were normalized against protein content. For promoter reporter assays, cells were cultured in 24-well plates and co-transfected with a promoter construct (I, II, III, or IV, as indicated in Fig. 5 and under "Results") plus pCMV-CREB or pSG5-CLOCK (150 ng each). pCDNA3.1 empty vector served as the control. Luciferase activity was determined as above.

TABLE 1
List of primers used to amplify the gga-mir-26a precursor and promoter (and mutations), gga-mir-124a precursor, and L-VGCCα1C 3′-UTR (and mutation)

PCR fragment	Primer	Sequence
gga-mir-26a precursor	Forward	5′-GGATCCATGTTAGCACGTCTGCTGTG-3′
	Reverse	5′-AAGCTTTGCCCGTGACATCTCAAGCTTCT-3′
gga-mir-124a precursor	Forward	5′-AGGCTCTGCCTCTCCGTGTTCACAG-3′
	Reverse	5′-AATGCCGCCTGGAGGATCCGCTCTT-3′
Chicken L-VGCCα1C 3′-UTR fragment	Forward	5′-ACTAGATTACAATCATAAGTCGTGTTGGC-3′
	Reverse	5′-TCTAGACTCAAACAAACTGAATTCGATTC-3′
Point mutation of chicken L-VGCCα1C 3′-UTR fragment	Forward	5′-GATGTTTCTGTTGAAGAAACCGTTATACT**aa**AATTCAGGTCAGTTTCGG-3′
	Reverse	5′-CCGAAACTGACCTGAATT**tt**AGTATAACGGTTTCTTCAACAGAAACATC-3′
2-kb gga-mir-26a promoter	Forward	5′-TATGAGCTCTTAACCTGTGATGTTCACTAGAAC-3′
	Reverse	5′-ACACTCGAGGTAACAGGATTAAGGAGTTTTGGC-3′
−150–+1(Δ−2kb−150) fragment of gga-mir-26a promoter	Forward	5′-TATGCTAGCTTGCTTGATATTAGTTGTTGAA-3′
	Reverse	5′-ACACTCGAGGTAACAGGATTAAGGAGTTTTGGC-3′
−2kb−300(Δ−300–+1) fragment of gga-mir-26a promoter	Forward	5′-TATGAGCTCTTAACCTGTGATGTTCACTAGAAC-3′
	Reverse	5′-AATGCTAGCTGCAGTGGTGGACACGGTTTAGC-3′

Quantitative Real Time PCR (Q-PCR)—The Q-PCR primers for the chicken L-VGCCα1C subunit were the same as previously described (19). The forward and reverse primers for chicken Bmal1 were 5′-ATACAGAAGCCAACTATAAGCCTGCT-3′ and 5′-CTGTAGTTGAGGATCTTGAAGACAGA-3′, respectively. The sequence for the 5′ fluorescent labeled oligonucleotide probe was 5′-AAATCCATCTGCTGCCCTGAG-3′ (Applied Biosystems). The QuantiMir Kit from SBI System Bioscience (Mountain View, CA) was used for Q-PCR detection of gga-mir-26a. Chicken E11 embryos were entrained *in ovo* under LD cycles for 6 days, and whole retinas were harvested at ZT 0, 4, 8, 12, 16, and 20. Total RNA was prepared by the RNeasy kit (Qiagen). The 3′ universal primer for Q-PCR was provided by the manufacturer. The 5′ primer for gga-mir-26a was 5′-TTCAAGTAATCCAGGATAGGC-3′. SYBR-green based Q-PCR master mix (Applied Biosystems) was used for PCR amplification (40 cycles). Reverse transcription (RT)-PCR amplification of the gga-mir-26a precursor was done at two time points, ZT 5 and ZT 17. The PCR primers were as follows: forward, 5′-GTCACCTGGTTCAAGTAATC-3′; reverse, 5′-GGTTACTTGCACTGGGAGGC-3′. The PCR fragments were separated on a 2.0% agarose gel, and band intensity was analyzed by Scion Image software.

Cell Culture, Biolistic Transfection, and Electrophysiology—Chicken retinas from E11 were dissociated, cultured, and entrained under LD cycles for 6 days and then kept in constant darkness (DD) in the presence of 40 ng/ml ciliary neurotrophic factor (R&D Systems, Minneapolis, MN) and 10% heat-inactivated horse serum, as described previously (32). On the last day of LD, cells were transfected using a biolistic particle delivery system (Helium Gene Gun; Bio-Rad) according to previous descriptions (26, 32). The plasmid encoding enhanced green fluorescent protein (eGFP) is commercially available (Vitality® hrGFPII-1 mammalian expression vector; Stratagene). In these experiments, gga-mir-26a or the empty vector was co-transfected with the GFP plasmid. After transfection, cells remained in culture under DD for a day before electrophysiological recordings were performed at night (ZT 16–19). Cardiomyocytes were dissociated and cultured from E12 embryos. The culture medium for cardiomyocytes contained Dulbecco's modified Eagle's medium and 10% fetal bovine serum. Conditions for transfection were the same for photoreceptors and cardiomyocytes.

The antagomir specifically targeting mature gga-mir-26a (anti-mir-26a) was purchased from Dharmacon (Thermo Scientific, Lafayette, CO). The sequence was 5′-$G_sC_sC_sU_sA_sU_s$-$C_sC_sU_sG_sG_sA_sU_sU_sA_sC_sU_sU_sG_sA$-3′. The subscript "s" represents a phosphorothioate linkage. Each nucleotide was modified by 2′-*O*-methylation, which allows the antagomir to function as an irreversible, stoichiometric inhibitor of targeted microRNAs (33). Transfections of anti-mir-26a were done by the same biolistic particle delivery system as described above with a molecular ratio of 20:1 to the phrGFPII-1 vector. In these experiments, chicken retina cells (E11) were cultured and LD entrained for 6 days as described earlier. Electrophysiological recordings were performed the day after transfection at ZT 4–8.

For retina electrophysiological recordings, perforated patch recordings of L-VGCCs were carried out as described previously (19, 32). The external solution contained the following: 110 mM NaCl, 10 mM $BaCl_2$, 0.4 mM $MgCl_2$, 5.3 mM KCl, 20 mM tetraethylammonium chloride, 10 mM HEPES, and 5.6 mM glucose, pH 7.4, with NaOH. The pipette solution was: 135 mM cesium acetate, 10 mM CsCl, 2 mM $MgCl_2$, 0.1 mM $CaCl_2$, 1.1 mM EGTA, and 10 mM HEPES, pH 7.4, adjusted with CsOH. β-Escin was prepared as a 50 mM stock solution in water and added to the pipette solution to yield a final concentration of 30–50 μM. Recordings were made from cone photoreceptors characterized morphologically as cells with elongated cell bodies with one or more prominent oil droplets. Recordings of cardiomyocyte L-VGCCs were performed using suction-formed whole cell patch configuration. The cardiomyocyte recording solutions were modified from Tohse *et al.* (34). The external solution was 145 mM tetraethylammonium chloride, 9 mM $BaCl_2$, 0.5 mM $MgCl_2$, 5.5 mM glucose, 0.1 mM $NiCl_2$, and 5 mM HEPES, pH 7.4, with CsOH or tetraethylammonium hydroxide. The pipette solution was 125 mM cesium acetate, 20 mM CsCl, 3 mM $MgCl_2$, 10 mM EGTA, and 5 mM HEPES, pH 7.4, adjusted with CsOH. The current density ($I_{density}$) was obtained by dividing the current amplitude by the membrane capacitance. Each group contained 9–18 cells.

All of the data are presented as mean ± S.E. Student's *t* test or one-way ANOVA followed by Tukey's *post hoc* test for unbalanced *n* were used for statistical analysis. *, $p < 0.05$ was regarded as significant throughout.

Immunocytochemistry—Retina cells after transfection on glass coverslips were fixed with Zamboni's fixative in phosphate buffer (PB; 0.1 mol/liter, pH 7.4) for 30 min at 22–24 °C and methanol at −20 °C for 20 min. Cells were washed in PB containing 0.1% Triton X-100, blocked with 0.1% Triton X-100/PB containing 3% normal goat serum for 1 h, and then incubated overnight with a primary antibody against VGCCα1C (Alomone, Jerusalem, Israel) at a dilution of 1:100. The next day, cells were washed with PB and incubated with a fluorescent conjugated secondary antibody (Alexa 594 nm goat anti-rabbit; Molecular Probes, Inc., Carlsbad, CA) in PB containing 1.5% normal goat serum for 1 h in the dark. After several washes in PB, the coverslips were mounted on a glass slide and stored at 4 °C for later observation on a Zeiss microscope with epifluorescence to determine the localization of L-VGCCα1C. The average fluorescence intensities per pixel (*F*) of the outlined structures were analyzed without any modification using the luminosity channel of the histogram function in Adobe Photoshop 6.0 (19, 26). Three cells (*F1*, *F2*, and *F3*) from each experiment were measured. The background fluorescence intensity was acquired from an adjacent area without any cells (*B*). The relative fluorescence intensity from one single image of a particular condition was converted as $((F1 - B) + (F2 - B) + (F3 - B))/3$. There were four repetitions for each condition, statistical comparisons were made using Student's *t* test, and $p < 0.05$ was regarded as significant. All fluorescence intensity analyses were carried out blind.

RESULTS

L-VGCCα1C Is a Downstream Target of mir-26a—To investigate the potential involvement of retinal miRNAs in the post-transcriptional regulation of the L-VGCCα1C subunit, several miRNA target prediction algorithms were applied for the primary screening process (available from the Memorial Sloan-Kettering Cancer Center microRNA, PicTar, and TargetScan Human web sites). We established several criteria to eliminate false positives. First, the miRNAs and the target site in the 3′-UTR must be highly conserved among humans, mice, and chickens. Second, the fist eight bases from the 5′-end of the miRNAs must perfectly complement the sequence of the target. Third, the free energy, Δ*G*, for the miRNA approach toward the target site cannot exceed −15 kcal/mol. Concurrently, Δ*G* from the flanking sequences of the target site (~40 bp) must be lower than miRNA targeting free energy (35, 36). This criterion reduced the possibility of mistakenly choosing miRNA whose binding to the target site could be impeded by the secondary structure of the flanking regions. Based on these criteria, we were able to narrow down our choices to nine miRNAs (mir-19a, mir-19b, mir-26a, mir-26b/mir-1297, mir-33, mir-96/mir-1271, and mir-155) of 150 predicted candidate miRNAs. Our last elimination criterion was that the candidate miRNA must be highly expressed in the retina. Recently, several miRNAs have been shown to be highly or specifically expressed in the eye (7, 37–39). MicroRNA-96 is exclusively expressed in the retina photoreceptor layer. However, although mir-26a is also expressed in other organs, it is more abundantly expressed in the mouse retina compared with other eye-specific miRNAs, including mir-96 (7). Therefore, we chose to investigate mir-26a as a possible regulator of L-VGCCα1C subunit expression in the retina. Since only a partial 3′-UTR was available from a predicted chicken L-VGCCα1C gene sequence (NCBI: XM_416388), we first confirmed that mir-26a targeted the chicken L-VGCCα1C 3′-UTR. The chicken L-VGCCα1C 3′-UTR was amplified by RT-PCR, sequenced (data not shown), and compared with the L-VGCCα1C 3′-UTRs of the human and mouse. The fragment derived from RT-PCR was ~0.8 kb. Homology comparison of the mir-26a target site within the L-VGCCα1C 3′-UTR among humans, mice, and chickens showed that this region is 100% conserved (Fig. 1*A*). *In vitro* reporter assays were performed to verify an interaction between mir-26a and the L-VGCCα1C 3′-UTR. The reporter construct containing the TK minimum promoter triggered luciferase expression. Four copies of the chicken L-VGCCα1C 3′-UTR target site (TK-Luc4XWT) were inserted between the luciferase stop codon and the SV40 poly(A) tail (Fig. 1*B*). The same reporter vector containing four copies of the point-mutated L-VGCCα1C 3′-UTR (TK-Luc-4Xmt) was used for the negative control. The luciferase assay results showed that gga-mir-26a repressed luciferase activity by 50–60% compared with the empty vector (Fig. 1*B*). A vector containing gga-mir-124a (positive control) did not show any inhibition of luciferase activity (Fig. 2*B*). Mutation of the L-VGCCα1C 3′-UTR target site (from 5′AAGAAACCGTTATACT**TG**AAT3′ to 5′AAGAAACCGTTATAC-T**aa**AAT3′) reversed the luciferase-repressive effects of gga-mir-26a (Fig. 1*B*). These reporter assays provided clear evidence that gga-mir-26a specifically targeted the 3′-UTR of the chicken L-VGCCα1C subunit.

gga-mir-26a Decreases L-VGCCα1C Protein Levels in Chicken Cone Photoreceptors—Since gga-mir-26a targeted the L-VGCCα1C 3′-UTR, we employed gene transfection and immunocytochemistry to investigate the functional regulation of L-VGCCα1C by gga-mir-26a in cone photoreceptors. Dissociated chicken retina cells were cultured and co-transfected with a mixture of gga-mir-26a expression vector and a vector (phrGFP-1) encoding eGFP. There are three features used to identify transfected chicken cone photoreceptors (*white arrows* in Fig. 2, *A–C*). First, avian cone photoreceptors contain oil droplets (*white arrowheads*) at the base of the outer segment. Other cells of the chicken retina do not have these oil droplets. Second, green fluorescent cells indicate positive transfections (Fig. 2, *A*, *B*, and *C*, *II*). Last, biolistic transfection delivers gold particles (*black arrowheads*) coated with expression vectors into the cells, and gene expression can be observed as early as 24 h after transfection. The L-VGCCα1C subunit was visualized by immunostaining with a specific antibody, which was mainly localized in the photoreceptor cell membrane (Fig. 2, *A–C*, *III*). The empty vector (pSilencer) was transfected as a negative control, whereas gga-mir-124a (pSilencer-mir-124a) was transfected as a positive control, since gga-mir-124a does not target L-VGCCα1C mRNA. The fluorescence overlay images show positively transfected cells with an empty vector (pSilencer), vector containing gga-mir-26a (pSilencer-mir-26a), or vector containing gga-mir-124a, as well as non-transfected cells (control; Fig. 2, *A*, *B*, and *C*, *IV*). There was no significant change in L-VGCCα1C fluorescence intensity between empty vector-transfected and non-transfected (control) cone

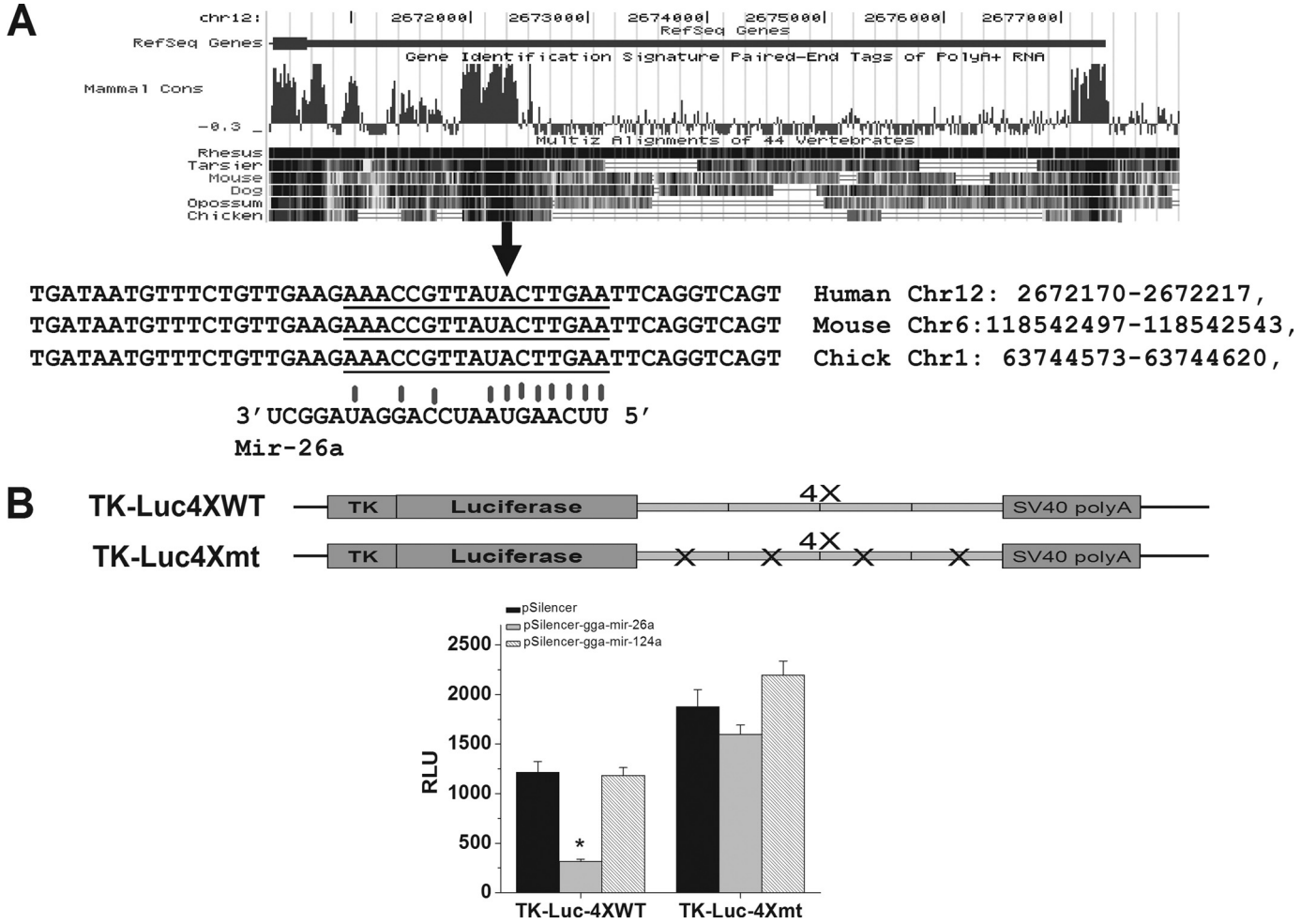

FIGURE 1. **gga-mir-26a targeted the 3′-UTR region of L-VGCCα1C mRNA.** *A*, the L-VGCCα1C 3′-UTR is highly conserved among humans, mice, and chickens. The *arrow* indicates the mir-26a target site. *B*, the naive (wild type) L-VGCCα1C 3′-UTR sequence containing the mir-26a target site was amplified, and four repeats were constructed into a pTK-Luc reporter vector (TK-Luc4XWT). The multimers with a selected point mutation in the L-VGCCα1C 3′-UTR mir-26a target sequence (TK-Luc4Xmt) was also constructed as negative controls for the same reporter assays. Luciferase reporter assays were performed after co-transfection with TK-Luc4XWT (*left*) or TK-Luc4Xmt (*right*) along with an empty vector (pSilencer; *black bars*), gga-mir-26a (pSilencer-gga-mir-26a; *light gray bars*), or gga-mir-124a (pSilencer-gga-mir-124a, positive control; *diagonal lined bars*). gga-mir-26a significantly inhibited the naive TK-Luc4XWT luciferase activity compared with the empty vector or gga-mir-124a. gga-mir-26a did not affect mutant TK-Luc4Xmt luciferase activity. $n = 5$ for each group. *, $p < 0.05$. *RLU*, relative luciferase units.

photoreceptor cells (Fig. 2*D*). Transfection with gga-mir-124a did not affect L-VGCCα1C expression in cone photoreceptors. On the other hand, L-VGCCα1C fluorescence intensity was significantly reduced (60%) in gga-mir-26a-transfected photoreceptor cells (Fig. 2*D*). Therefore, gga-mir-26a negatively regulated the L-VGCCα1C subunit protein level in chicken cone photoreceptors.

gga-mir-26a Down-regulation of L-VGCCα1C Subunits in Turn Diminishes L-VGCC Current Amplitudes—Previously, we showed that there is a circadian regulation of L-VGCC currents in cone photoreceptors, with maximal current amplitudes during the subjective night (19). The circadian regulation of cone L-VGCC current amplitude is partially attributed to higher expression of L-VGCCα1D subunits during the subjective night. Inhibition of the ERK-mitogen-activated protein kinase-calcium-calmodulin kinase II signal transduction pathway dampens the circadian rhythm of L-VGCCs. Here, we showed that the down-regulation of the L-VGCCα1C subunit by gga-mir-26a caused a concomitant decrease in L-VGCC current amplitudes in chicken cone photoreceptors. Chicken cone photoreceptors were cultured and entrained for 6 days under 12:12 h LD cycles, and on the last day of LD, cells were transfected with either empty vector or gga-mir-26a expression vector and kept in DD for another 24 h before patch clamp electrophysiological recordings. Recordings were only performed on photoreceptors expressing eGFP at night (ZT 16–19). The current density-voltage (*I*-V) relationship of individual photoreceptors transfected with empty vector (control) or gga-mir-26a (mir-26a) is shown in Fig. 3*A*. The average maximum current density of photoreceptors transfected with an empty vector (control) or gga-mir-26a was 8.8 ± 0.9 pA/pF and 3.05 ± 0.6 pA/pF, respectively (Fig. 3*E*). There was no change in the voltage that elicited maximum current amplitudes between controls and gga-mir-26a-transfected cells (Fig. 3, *B* and *E*). This result indicated that gga-mir-26a did not change the channel activation mechanism of L-VGCCs. Instead, the decrease in L-VGCC current density resulted from the repressive action of gga-mir-26a on the expression and/or insertion of L-VGCCα1 subunits. Collectively, these results led us to conclude that gga-mir-26a inhibited L-VGCC

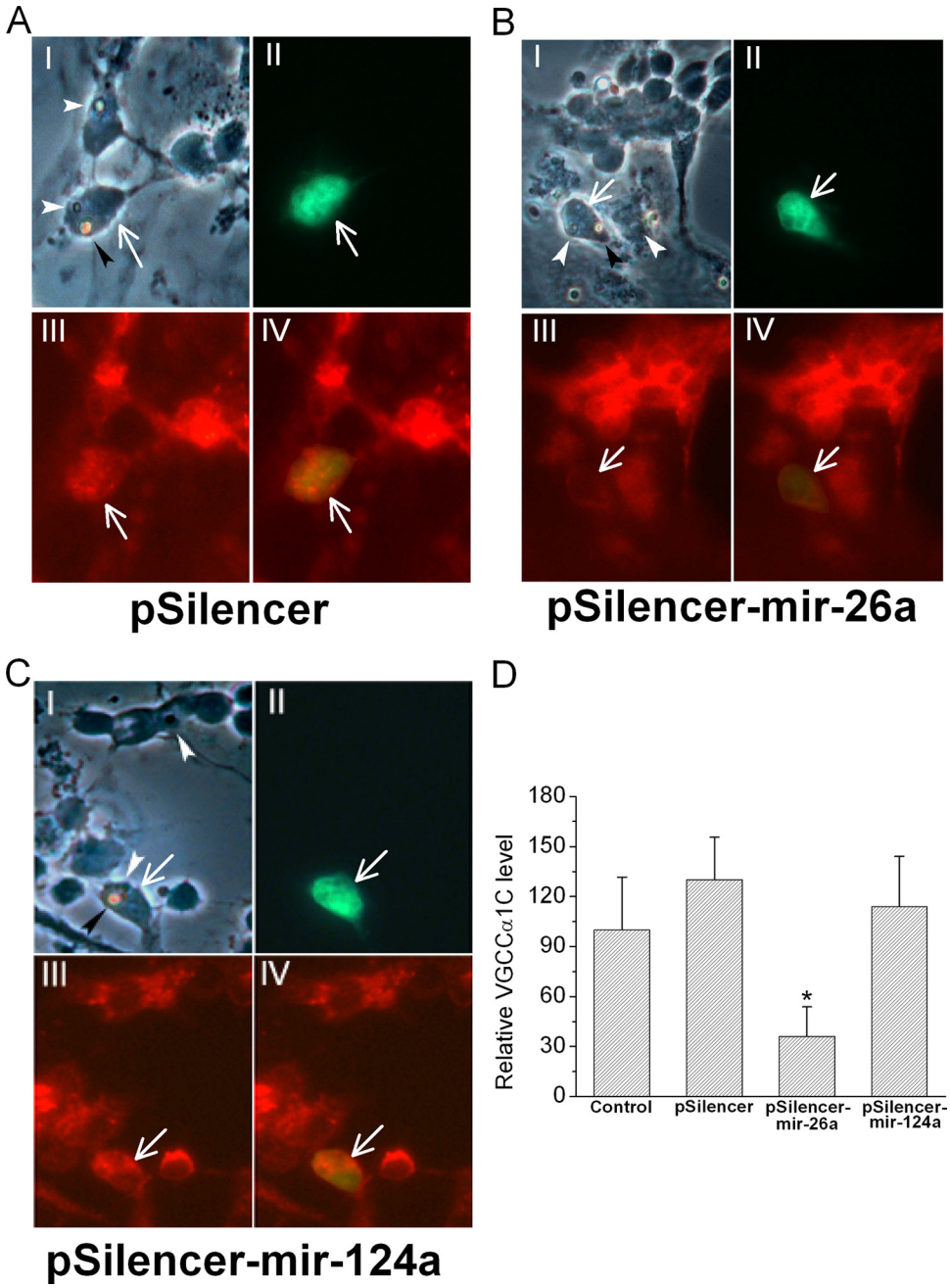

FIGURE 2. **Overexpression of gga-mir-26a reduced L-VGCCα1C expression in chicken cone photoreceptors.** Chicken cone photoreceptors were co-transfected with a plasmid encoding eGFP and empty vector (*pSilencer*; *A*) (negative control), gga-mir-26a (*pSilencer-mir-26a*) (*B*), or gga-mir-124a (*pSilencer-mir-124a*; *C*) (positive control). *I*, phase-contrast images of cone photoreceptors; the *white arrowheads* indicate the oil droplets, and the *black arrowheads* indicate the gold particles used for biolistic transfection. The *white arrows* indicate the cone photoreceptors that were positively transfected. *II*, expression of eGFP in transfected photoreceptors (*white arrows*). *III*, immunocytochemical staining of L-VGCCα1C; the *white arrows* indicate photoreceptors that were positively transfected. *IV*, overlay images of both eGFP- and L-VGCCα1C-positive. *D*, the fluorescence intensity of L-VGCCα1C was quantified. There was no difference in L-VGCCα1C fluorescence intensity between control (non-transfected) photoreceptors, photoreceptors transfected with empty vector, or photoreceptors transfected with gga-mir-124a. In gga-mir-26a-transfected cone photoreceptors, there is a significant decrease in L-VGCCα1C fluorescence intensity, whereas transfection with gga-mir-124a has no effect on the expression of L-VGCCα1C. Each group contained four trials. *, $p < 0.05$.

activities through down-regulation of L-VGCCα1C subunit expression in chicken cone photoreceptors. To rule out the possibility that the down-regulation of L-VGCCs by gga-mir-26a was caused by other indirect pathways exclusively found in cone photoreceptors, we tested whether gga-mir-26a modulated L-VGCCs in chicken cardiomyocytes. The L-VGCCα1C is highly expressed in cardiomyocytes and is responsible for the control of cardiac contraction force during excitation-contraction coupling (40), and mir-26a is also abundantly expressed in mammalian hearts (5). Chicken E12 cardiomyocytes were cultured *in vitro* for 2 days until the cells started to pulse. Whole cell patch clamp electrophysiological recordings were performed 24 h after cardiomyocytes were transfected with an empty vector (control) or gga-mir-26a. The *I*-V relationships recorded from transfected cardiomyocytes were similar to those of cone photoreceptors, in which cardiomyocytes transfected with gga-mir-26a had a significant decrease in L-VGCC current amplitude and density (Fig. 3, *C–F*). The average maximum current density of cardiomyocytes transfected with control or gga-mir-26a vectors was 31.8 ± 5.4 pA/pF and 15.7 ± 2.5 pA/pF, respectively. This result confirmed the conclusion that gga-mir-26a specifically targeted and repressed the expression of L-VGCCα1C subunits and caused a significant decrease in current density.

Anti-mir-26a, a Specific gga-mir-26a-targeting RNA Oligonucleotide, Reverses the Inhibitory Effect of gga-mir-26a and Increases L-VGCC Activity during the Subjective Day—If gga-mir-26a does indeed target and repress the expression of L-VGCCα1C, inhibition of gga-mir-26a should reverse this repression. Since the L-VGCC current is under circadian control in cone photoreceptors, and the current is smaller during the subjective day (19), it is possible that the smaller L-VGCC day current is due to the repressive action of gga-mir-26a. If so, inhibition of gga-mir-26a during the day would increase the L-VGCC currents. We chose to use an antagomir specifically against mature gga-mir-26a to test our hypothesis. Each nucleotide of the antagomir was phosphorothioate-linked and 2′-*O*-methylated to ensure pairing stability and specificity. Photoreceptors, after culture and LD entrainment, were co-transfected with eGFP and either an empty vec-

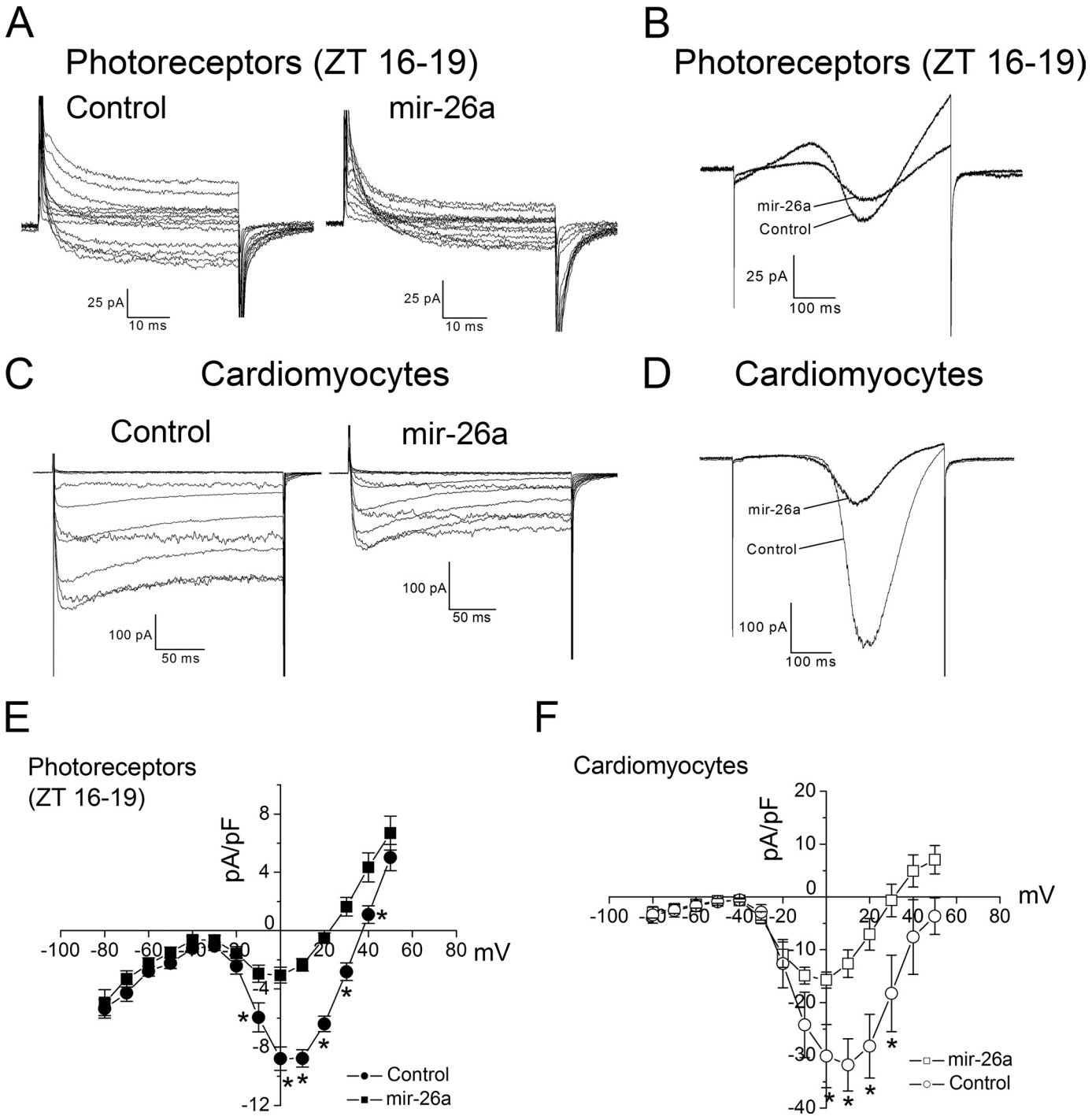

FIGURE 3. **gga-mir-26a repressed L-VGCC current amplitudes.** Photoreceptors (*A*, *B*, and *E*) or cardiomyocytes (*C*, *D*, and *F*) were co-transfected with eGFP and either the empty vector (control) or gga-mir-26a. *A*, *B*, and *E*, after 24 h in DD, perforated patch recordings were performed on photoreceptors only at night (ZT 16–19). Two representative recordings from photoreceptors transfected with empty vector (control) or gga-mir-26a (*A* and *B*). *A*, cells were held at −65 mV, and step commands were given from −60 to +50 mV at 10-mV intervals in 50 ms. *B*, a ramp command was given from −80 to +60 mV over 500 ms. *E*, the average current density (pA/pF)-voltage (mV) relationship obtained from step commands of control (*solid circle*) or gga-mir-26a (*solid square*) transfected photoreceptors were plotted. $n = 9$ for the control, and $n = 8$ for mir-26a; *, $p < 0.05$ in Student's *t* test. Whole cell patch recordings from two representative cardiomyocytes were transfected with empty vector (control) or gga-mir-26a (*C* and *D*). *C*, cells were held at −65 mV, and step commands were given from −60 to +50 mV at 10-mV intervals in 200 ms. *D*, a ramp command was given from −80 to +60 mV over 500 ms. *F*, the average current density (pA/pF)-voltage (mV) relationship of control (*open circle*) or mir-26a (*open square*) transfected cardiomyocytes was plotted. $n = 8$ for both control and mir-26a groups; *, $p < 0.05$ in Student's *t* test.

tor (control) or the gga-mir-26a antagomir (anti-mir-26a). After 24 h in DD, perforated patch recordings were performed on photoreceptors only during the day (ZT 4–8). The current density-voltage (*I*-V) relationship of individual photoreceptors transfected with an empty vector (control) or anti-mir-26a is shown in Fig. 4*D*. The average maximum current density of photoreceptors transfected with an empty vector (control) or anti-mir-26a was 4.9 ± 0.7 pA/pF and 8.0 ± 0.6 pA/pF, respectively (Fig. 4*D*). There was no change in the voltage that elicited maximum current amplitudes between control and anti-mir-

26a-transfected cells (Fig. 4*D*). The increase in L-VGCC current density resulted from down-regulation of gga-mir-26a by anti-gga-mir-26a during the day (ZT 4–8). This anti-gga-mir-26a-mediated increase in L-VGCC current density was blocked by the specific L-VGCC inhibitor nitrendipine (3 μM; Fig. 4*C*). In the experiments outlined above, we showed that gga-mir-

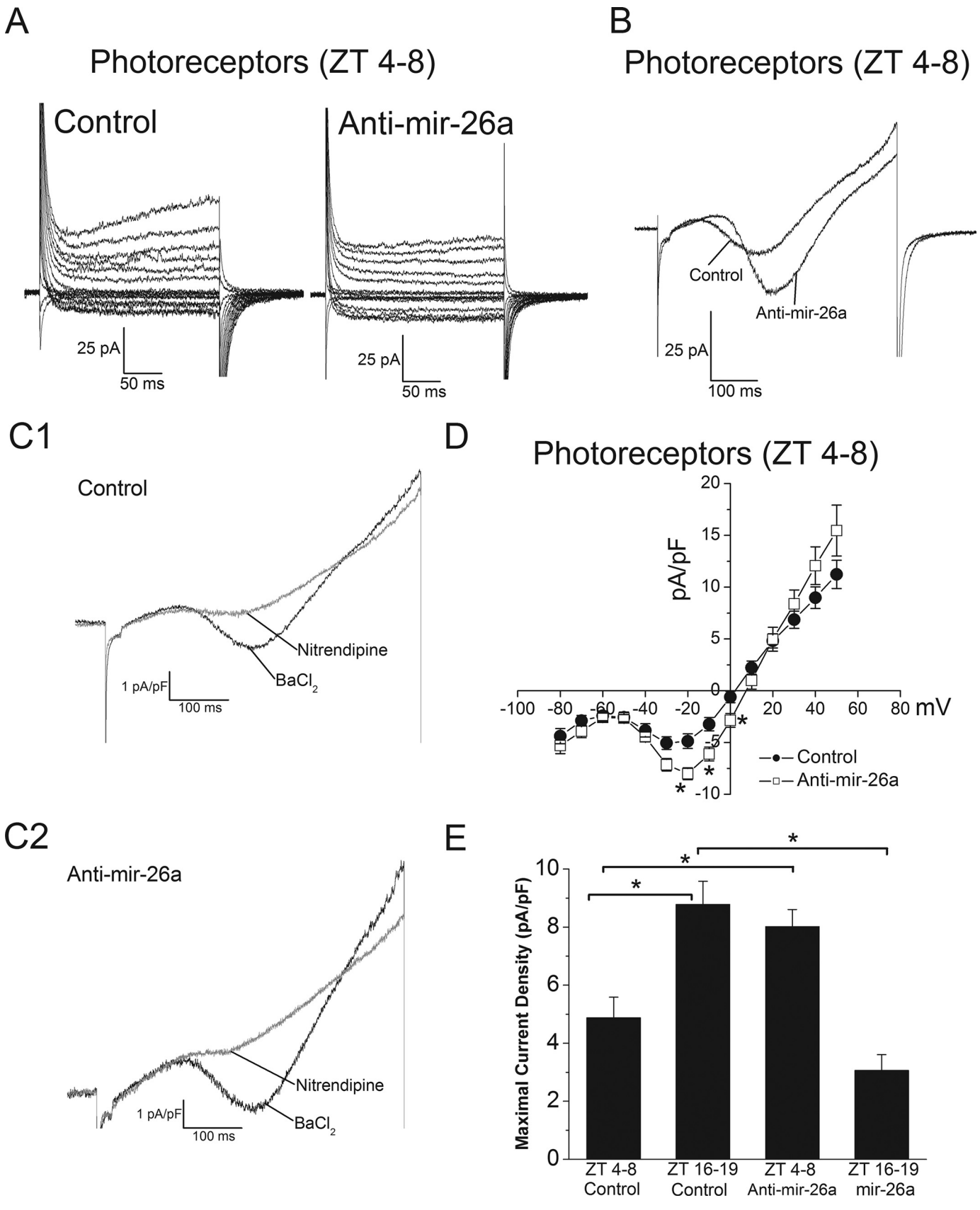

26a inhibited L-VGCC activities through down-regulation of L-VGCCα1C subunit expression in chicken cone photoreceptors (Figs. 2 and 3). Since inhibition of gga-mir-26a during the day (ZT 4–8) increased L-VGCC currents, whereas transfection with gga-mir-26a repressed L-VGCC currents at night (ZT 16–19; Figs. 3*E* and 4*E*), we postulated that the expression of gga-mir-26a might play a role on the circadian regulation of L-VGCCα1C in chicken cone photoreceptors.

The Expression of gga-mir-26a in Chicken Retina Is under Circadian Control—Previous studies of miRNA expression indicated that mir-26a is highly expressed in the mouse retina, and its expression is under circadian control, which is higher during the day and lower at night (5, 8). However, detailed biological functions of mir-26a remained to be explored. Sequence alignment among five species indicates that mir-26a, and possibly its biological functions, is highly conserved (Fig. 5*A*, *top*). We used RT- and Q-PCR to investigate the expression and functional role of precursor and mature gga-mir-26a. Chicken embryos at E11 were LD-entrained (12 h/12 h) *in ovo* for 5–6 days. Retinas were harvested at ZT 5 (day) and ZT 17 (night). Total RNA was carefully isolated to avoid genomic DNA contamination. Reverse transcription PCR was used for the detection of gga-mir-26a precursor. We found that there was a daily rhythm in gga-mir-26a precursor expression with higher expression at ZT 5 and lower expression at ZT 17 (Fig. 5*A*, *bottom*). There was at least a 3-fold difference between the two time points. The expression of mature gga-mir-26a was quantified by Q-PCR at six different time points (ZT 0, 4, 8, 12, 16, and 20). Similar to its precursor, mature gga-mir-26a peaked at ZT 4, which was significantly different from the other time points (Fig. 5*B*). The peak level of gga-mir-26a was at least 4-fold greater than the trough level. Chicken Bmal1 mRNA expression was used as a positive control and showed a diurnal rhythm with a peak at ZT 8 and nadir at ZT 20 (Fig. 5*B*). The peak Bmal1 mRNA level was about 7-fold more than the trough level. This result was comparable with previous reports (23, 41). The L-VGCCα1C mRNA level peaked at ZT 12, which was during the transition period from light to dark (Fig. 5*B*). However, the amplitude of the L-VGCCα1C mRNA rhythm was small and considered a weak rhythm, since the peak was only 2.5 times that of the trough. Previously, we showed that the mRNA levels of L-VGCCα1C do not display a circadian rhythm under DD, whereas the mRNA of VGCCα1D is under circadian control in the chicken retina. However, the protein expression of both L-VGCCα1C and α1D subunits are higher during the subjective night than the subjective day in cone photoreceptors

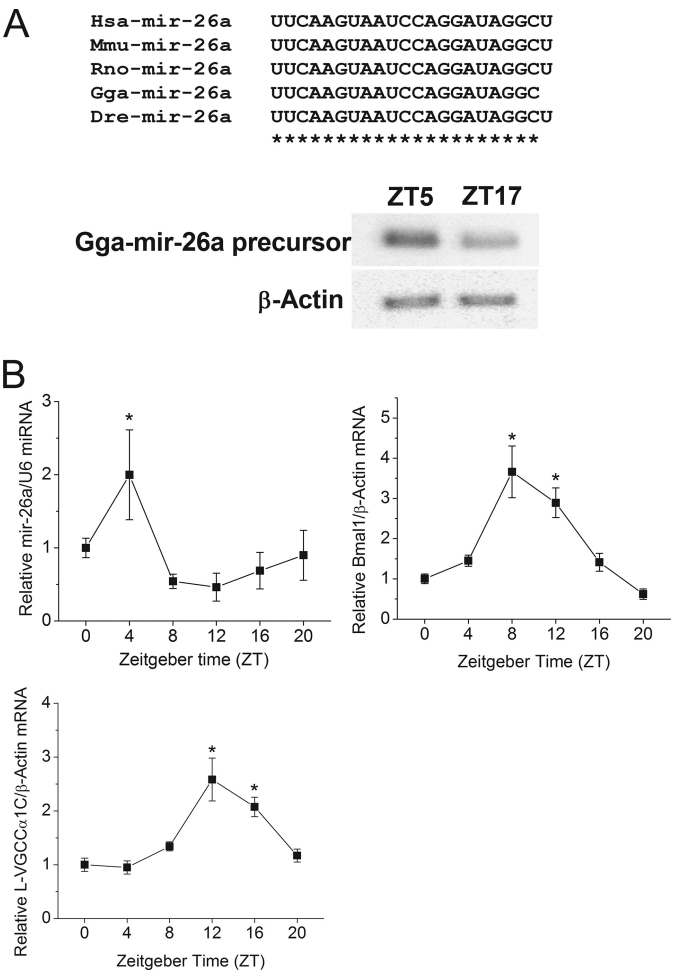

FIGURE 5. **There was a diurnal expression of gga-mir-26a in the chicken retina.** *A*, the *top* shows the sequence alignment of mature mir-26a among human (*Hsa*), mouse (*Mmu*), dog (*Rno*), chicken (*Gga*), and *Drosophila* (*Dre*). *, identical nucleotides. The *lower panel* shows the RT-PCR amplification of gga-mir-26a precursor from the chicken retina harvested at ZT 5 (day) and ZT 17 (night). β-Actin served as an internal control. *B*, there were diurnal expressions of mature gga-mir-26a (mir-26a) and mRNAs of Bmal1 and L-VGCCα1C in the chicken retina. *Upper left*, gga-mir-26a reached its highest levels at ZT 4, which was significantly different from the other five time points ($n = 5$ for each time point; *, $p < 0.05$). *Upper right*, the mRNA levels of Bmal1 at ZT 8 and 12 are significantly different from ZT 0, 4, 16, and 20 ($n = 6$ for each time point; *, $p < 0.05$). *Lower left*, the mRNA levels of L-VGCCα1C at ZT 12 and 16 are significantly higher than ZT 0, 4, 8, and 20 ($n = 6$ for each time point; *, $p < 0.05$).

(19). Therefore, we postulated that there might be a posttranscriptional regulation of L-VGCCα1C protein expression, in which either its mRNA was specifically broken down to smaller

FIGURE 4. **Anti-gga-mir-26a increased L-VGCC current amplitudes.** Photoreceptors were co-transfected with eGFP and either the empty vector (control) or an antagomir specifically against gga-mir-26a (anti-mir-26a). After 24 h in DD, perforated patch recordings were performed on photoreceptors only during the day (ZT 4–8). Shown are two representative recordings from photoreceptors transfected with empty vector (control) or anti-mir-26a (*A* and *B*). *A*, cells were held at −65 mV, and step commands were given from −60 to +50 mV at 10-mV intervals in 50 ms. *B*, a ramp command was given from −80 to +60 mV over 500 ms. *C*, the L-VGCC current densities recorded from naive photoreceptors (*Control*) or photoreceptors transfected with anti-mir-26a were blocked by extracellular administration of an L-VGCC inhibitor, nitrendipine (3 μM). *D*, the average current density (pA/pF)-voltage (mV) relationship obtained from step commands of control (*solid circle*) or anti-mir-26a (*open square*) transfected photoreceptors was plotted. $n = 11$ for the control, and $n = 12$ for anti-mir-26a; *, $p < 0.05$ in Student's *t* test. *E*, the maximal current densities of L-VGCCs were compared among four different groups: control photoreceptors recorded during the day (ZT 4–8), control photoreceptors recorded at night (ZT 16–19), anti-mir-26a-transfected photoreceptors recorded during the day (ZT 4–8), and mir-26a-transfected photoreceptors recorded at night (ZT 16–19). There is a diurnal regulation of L-VGCCs, and the maximal current density recorded during the day (ZT 4–8) is significantly different from the photoreceptors recorded at night (ZT 16–19). Recordings from cells transfected with anti-mir-26a during the day (ZT 4–8) have a significant increase in maximal L-VGCC current density compared with the day controls. Recordings from cells transfected with mir-26a at night (ZT 16–19) have a significant decrease in maximal L-VGCC current density compared with the night controls. The ZT 16–19 control and mir-26a data are the same from Fig. 3*E*. Comparisons were made by one-way ANOVA with Tukey's *post hoc* test; *, $p < 0.05$.

fragments or protein translation was inhibited at specific circadian times. We also suspected that retinal miRNAs might be involved in the circadian regulation of L-VGCCα1C in chicken cone photoreceptors because of the molecular nature of miRNAs. As a new posttranscriptional and translational regulatory mechanism, miRNAs can knock down the protein levels translated from downstream genes, whereas overall mRNA levels of the targeted genes remain relatively constant (36, 42, 43). The peak level of gga-mir-26a was a few hours ahead of the peak mRNA levels of Bmal1 and L-VGCCα1C. This observation led to the possibility that there is an underlying regulatory mechanism between gga-mir-26a and L-VGCCα1C in the chicken retina.

Circadian Expression of gga-mir-26a Is Regulated by Both CLOCK and CREB—Circadian oscillators in the retina regulate visual sensitivity and retinal physiology and function (13). Multiple elements composing the circadian oscillators (molecular clocks) or participating in the input and output pathways, including Clock/Bmal1, Per1/Per2, Cry1/Cry2, casein kinase 1, adenyl cyclase 1, and cAMP, have been found to be rhythmically expressed in vertebrate retinas (23, 44–47). Although the details of the molecular mechanisms generating circadian rhythmicity vary among species, in chicken photoreceptors, CLOCK/BMAL1 and light-driven cAMP signaling play a major role in regulating the transcription of circadian genes (48). Above, we described the circadian expression of gga-mir-26a. To further delineate the mechanism underlying the circadian regulation of gga-mir-26a expression and identify the key circadian regulators responsible for its rhythm, we performed promoter reporter assays. We amplified and analyzed (p-Match, Biobase) a 2-kb region directly upstream of the gga-mir-26a promoter (Fig. 6, *A* and *B*). Two transcriptional *cis* elements intricately involved in circadian regulation were identified from the gga-mir-26a promoter region. Two CRE elements (-TGAT-GGCA-) were located −1273 bp (−) and −681 bp (+) upstream of the gga-mir-26a promoter (Fig. 6, *A* and *B*). These CRE sequences were 75% identical to the typical consensus palindromic CRE: TGACGTCA with only 2 bp different. However, it has been reported that CREB transcriptional factors can bind to this variant sequence (-TGATGGCA-) and transactivate the downstream target gene even if the binding affinity is lower than to the consensus sequence (-TGACGTCA-) (49). In addition, there were two E-box elements (-CANNTG-) in close proximity to the gga-mir-26a promoter, −229 bp (+) and −187 bp (+) (Fig. 6, *A* and *B*). CLOCK and Bmal1, among other transcription factors, contain a helix-loop-helix protein structural motif that allows them to bind to E-box elements or related variant sequences to regulate transcription of the downstream genes. Since activities of both CREB and CLOCK are rhythmic and participate in the circadian regulation of mouse photoreceptor and SCN function (50, 51), the circadian expression of gga-mir-26a in chicken cone photoreceptors could be regulated by both transcriptional factors. Deletions of E-box (II and IV) or both CRE and E-box (III) in the gga-mir-26a promoter region were constructed and tested using the luciferase reporter assay (Fig. 6*B*). One of four reporters, the whole −2 kb gga-mir-26a promoter region (I) or the −2 kb promoter region with E-box deletion (Δ−300–150 and Δ−150–+1; II and IV) or CRE and E-box deletion (−150–+1; III), was co-transfected with either empty vector (pCDNA3.1), pCMV-CREB, or pSG5-CLOCK into COS1 cells (Fig. 6*C*, *bottom*). Both CLOCK and CREB were obtained from Mammalian Gene Collection clones, but there is 85% homology between mouse and chicken CLOCK and 98% homology between mouse and chicken CREB. Hence, mouse CLOCK and CREB can serve the same functions as the chicken homologs. CLOCK was slightly more effective than CREB, but both enhanced gga-mir-26a expression, as determined by a luciferase reporter assay (Fig. 6*C*, *I*). Deletion of the E-box(es) in the gga-mir-26a promoter region (as indicated in *II*, *III*, and *IV*) significantly decreased the transcription regulatory activity by CLOCK, and the activities of CREB were diminished once the CRE elements were deleted (as indicated in *III*). Hence, gga-mir-26a was a downstream target of both CLOCK and CREB.

DISCUSSION

In retina photoreceptors, CNGCs and L-type VGCCs have been the most vigorously studied ion channels in regard to their gating properties and physiological functions. The CNGCs are non-selective cation channels that belong to a family of cyclic nucleotide-gated channels. The CNGCs carry the photoreceptor "dark current" and serve essential roles in the light-dependent changes in photoreceptor membrane potential and subsequent neural processing (52). The L-VGCCs mediate a voltage-dependent, depolarization-induced calcium influx that governs neurotransmitter release from retinal photoreceptors (28). Both of these channels are circadian regulated (18, 19). In chicken cone photoreceptors, the apparent affinity of CNGCs to cGMP is higher during the subjective night than the subjective day, whereas the maximum current amplitude does not change throughout the day (18, 53). Conversely, the L-VGCC maximum current amplitudes as well as the functional expression of L-VGCCα1D are significantly higher during the subjective night (19, 26). A common mechanism underlying the circadian regulation of both channels is the Ras-ERK signal transduction pathway. Blockage of this signal transduction pathway dampens the circadian rhythm of CNGCs and L-VGCCs. However, there is no obvious circadian change of L-VGCCα1C mRNA levels in the chicken retina, but the protein levels of the L-VGCCα1C subunit in chicken cone photoreceptors were higher at night. There are three major VGCCα1 subunits that are expressed in the retina: α1C, α1D, and α1F (19, 54). Whereas L-VGCCα1D and α1F are highly expressed in photoreceptors relative to other retinal cells (54), the α1C subunit is expressed in all types of retinal cells, including ganglion cells, amacrine cells, bipolar cells, and glia cells (19). The regulation of L-VGCCα1C expression may vary among retinal cell types. This distinct possibility may be part of the reason that the overall protein expression of L-VGCCα1C is not rhythmic in chicken whole retina (19). However, it appears that there is a posttranscriptional regulatory mechanism underlying the circadian regulation of L-VGCCα1C protein level in the chicken cone photoreceptor, as we show in this study and discuss below.

In this report, we showed that gga-mir-26a regulated the protein level of the L-VGCCα1C subunit in chicken cone

A

```
-1120
ATGTGTGAACAGTGGAGCTGTGCCATCAGTAGCGCATCCTATCTGCCTTAGGTAGAACCCCATGGAAAAC
AAATGGAGAACAAGCTTTCAGAAGTGCCCTTTTGGAAGGAAATCTGACTCAGGTCTTCTTCAGATCTCGT
ATACCAGAGTTACTTCTACGTGGTGAATTTGTGTTTGCCCCTGTGTTGCTGTACGCTTCCAAGAGATTTC
ATACTGACTTATCTAACAAGTTTTGTTTATGGTACATATTGTATTCTTTGTTGTTATGCAGCAAAGTCAT
TCAAAAAGACTTATCTTGAATTTGGGGTGTTTTTATCCCTTTCTACTGTGTAATCCAGAGGTCAAAGAAG
CTTTTACTCTCCTACAGAAAGGTCCATTGGATCATTGTCTTGGGTAAACCAGCTTCCTTAGATTAAAGAA
AATAGCTTTTCTGAACCCCCCTTGGGCCTCTTCCATCTTTCCATCTCTTGTTAGAAAGGATTTGCCATTT
AATTTTACAAGGAAATAACTGATGTGAAGGACCTGTTGTTCCTGCTGCTGGAGGTGTTCAGATGCCTACA
GAGGCTGTAAGCTTGTGTTCCTGGGCATGAATTCCCCACATTGTGTTGGCAATGATGGCACAGATTTAAA
AAGCAAAAATTAACACAAACTGACATTATTTTGGCCAGTTCTCTTAATTTCTTTTCGCTTCTCTGAATGA
AAGGAAATCAGAGCTGGTCCCCTGTTCTGCCAAAGTATAAGCGAGGAACTGTGGGAAGTGCAGTGGAATG
TGTTGCAACTGAGACTTGAATGCTCTTCAGAGGGAGTTAATTGAGGGTGAAAGTAGTGGTTGCAGAAAAG
ATGTTCAACCTGGTTGGTACCCTGACAGAACTTCTGCAGGATCGCGTTCTCTCTCCTTGAGCGTGCTTCC
CATTCATAGGATCACAGAGAGCCATGAAGATTGGAAAAGACCTCCAAGGTCATTTGGTCCAACCATCAGC
CCATCACCACCATGCCTGCTAAACCGTGTCCACCACTGCACCACTTCCCTGGGCACGCTGTCCCACCGCG
TTTTGGTTTGGTGTCACCTGCAATTTTGTCCCTGAATGTAACTCGTTTATTAATTGCAACTGTATTTTAA
GTGGTTTTTATATCAGTTAATAATTGCTTGATATTAGTTGTTGAAAGATAAAGAGATGTTAGCACGTCTG
CTGTGAATGTAATGTACAAAATGTTCTTTAATGTCGGGAGCAAATGCCATTCAAATAATACACTTTATTT
TCTATGACGGCCAAAACTCCTTAATCCTGTTAC
-173
```

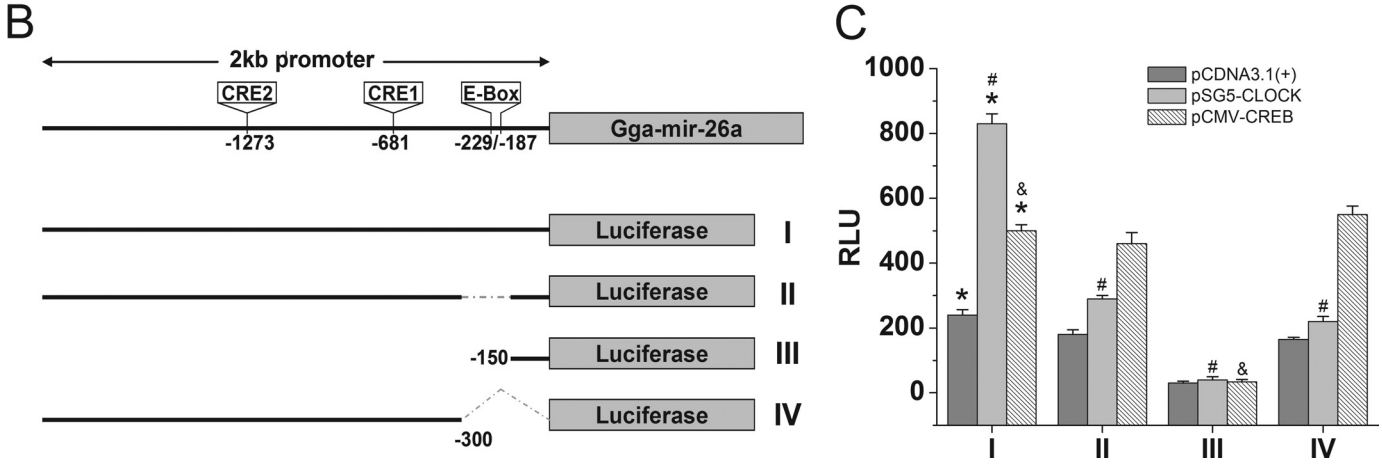

FIGURE 6. **CLOCK and CREB enhance gga-mir-26a expression *in vitro*.** The luciferase reporter assays were performed by co-transfecting COS1 cells with one of the four reporter constructs (*I*, *II*, *III*, or *IV*) with either empty (pCDNA3.1), CLOCK (pSG5-CLOCK), or CREB (pCMV-CREB) expression vector. *A*, the sequence upstream of the gga-mir-26a promoter region (−1120 to −173) contained two CRE (*italic type*) and two E-box (*italic* and *underlined type*) *cis* elements. *B*, schematic diagram of the four luciferase reporter constructs of the gga-mir-26a promoter region: luciferase reporter with the 2-kb gga-mir-26a promoter region (*I*); 2-kb promoter region with a deletion mutation of E-box binding sites (Δ−330 to −150) (*II*); shorter promoter region with CRE and E-box deletion mutations (−150 to +1) (*III*); another E-box deletion mutation within the promoter region from −2 kb to −300 (*IV*). *C*, relative luminescence intensity (*RLU*) from the luciferase reporter assay after co-transfection with one of the four reporter constructs (*I*, *II*, *III*, or *IV*) and empty vector pCDNA3.1 (*dark gray*), pSG5-CLOCK (*light gray*), or pCMV-CREB (*diagonal lines*). Luciferase reporter assay results showed that CLOCK enhanced gga-mir-26a expression 3-fold, whereas CREB increased it 2-fold. Deletion of E-box (*II*, *III*, and *IV*) or both E-box and CRE (*III*) elements in the gga-mir-26a promoter region significantly reduced the transcriptional activities by CLOCK and CREB transcriptional factors. The empty vector pCDNA3.1 served as a control. $n = 5$ for each group. *, significant differences in RLU between pSG5-CLOCK or pCMV-CREB and pCDNA3.1 when co-transfected with full-length gga-mir-26a (*I*). #, significant decreases in RLU when pSG5-CLOCK is co-transfected with II, III, or IV compared with co-transfection with I. &, significant decrease in RLU when pCMV-CREB is co-transfected with III compared with co-transfection with I. $p < 0.05$.

photoreceptors. As a group of non-coding small RNAs, miRNAs participate in diverse biological processes, such as cell proliferation and differentiation, development, and carcinogenesis, and as the cause of some neuronal diseases (55–58). MicroRNAs are also involved in the regulation of circadian rhythm in the mouse SCN (6). The transcription of miRNA precursors can be accomplished by either RNA polymerase II or III, and the transcription of miRNAs is controlled by multiple *cis* elements and trans-activators in the promoter region (1). MicroRNAs exhibit specific temporal and spatial expression following environmental stimulation (59), and they repress gene expression through complementary binding to the 3′-UTR of mRNAs. There are several miRNA candidates that can potentially down-regulate L-VGCCα1C expression, but only mir-26a is highly expressed in the retina and under circadian regulation (5). MicroRNA-26a has been discovered in muscle, heart, and neuronal cells, and it has been recently reported that several genes are downstream targets of mir-26a in different tissues, such as enhancer of Zeste homolog 2 during myogenesis (60) and Sma- and Mad-related protein 1 transcriptional factor in osteogenic differentiation of human adipose tissue-derived stem cells (61). Since a single miRNA can target several different genes, each miRNA often has diverse functional roles (1). It is possible that mir-26a might have additional functions other than the modulation of L-VGCCα1C in the retina, as our results show.

Here, we demonstrated that gga-mir-26a directly targeted the 3′-UTR of L-VGCCα1C subunit mRNAs, thereby decreasing L-VGCCα1C subunit expression. Interestingly, both CLOCK and CREB enhanced the expression of gga-mir-26a. In the chicken retina, both Clock and Bmal1 mRNA levels peak at the light-dark transition (23, 41), whereas the cAMP level is lowest in the morning and reaches its pinnacle late at night (16). Elevated cAMP leads to activation of the CREB transcriptional factor through a protein kinase A-dependent phosphorylation of CREB transcriptional factor (62). The phosphorylated CREB transcriptional factor further activates rhythmic expression of several genes, such as the melatonin-synthesizing enzyme, arylalkylamine *N*-acetyltransferase, and Period 2 (63, 64). Hence, cAMP-induced activation of CREB transcriptional factor could be the major activator responsible for higher gga-mir-26a expression during the daytime, which was consistent with our result showing mature gga-mir-26a levels being higher during the day in the chicken retina. It appears that both CLOCK and CREB may regulate the L-VGCCα1C subunit through gga-mir-26a in chicken cone photoreceptors.

The molecular mechanism of the core oscillator (the "molecular clock") has been based on two interlocking transcription-translation feedback loops: one is the Clock/Bmal1-Pers negative feedback loop, and the other is the Clock/Bmal1-REV-ERBα feedback loop (65, 66). Other epigenetic modifications of the circadian oscillator, such as phosphorylation, acetylation, and ubiquitination, have also been documented to play important parts in the regulatory mechanisms of the molecular clock (67–69). As an additional transcriptional and translational regulatory mechanism, several miRNAs have been discovered to participate in the molecular clock (2, 3, 5). The mir-182–96 cluster in the mouse retina is a downstream target of the CLOCK transcriptional factor (5), whereas mir-132 and mir-219 are involved in circadian entrainment in the SCN (6). Since the expression of miRNAs is also under the regulation of its own promoters and related transcriptional factors, miRNAs could potentially serve in both circadian input entrainment and output pathways. Circadian regulated miRNAs could serve as the link between the core oscillators and output signaling that further governs biological functions. In summary, we showed that gga-mir-26a served as part of the circadian output and modulated L-VGCCα1C expression in cone photoreceptors. Evidently, there could be multiple mechanisms underlying the circadian regulation of different L-VGCC subunits. Therefore, we do not exclude the possibility that there might be several regulatory mechanisms at work on one L-VGCC subunit at different molecular levels from transcription and translation to post-translational modifications. In addition to mir-26a, other miRNAs are also highly expressed in the retina, but the biological functions of these miRNAs are still not clear. The circadian regulation of various miRNAs suggests that there are more potential posttranscriptional regulators in circadian oscillator-controlled protein expression. Our work has shed new light on the mechanism underlying the circadian regulation of photoreceptor function. The functional roles of miRNAs in the molecular clock as well as the circadian input/output pathways are worthy of future exploration and investigation.

Acknowledgments—We are very grateful for the comments from Drs. Deborah Bell-Pederson, Paul Hardin, and Terry Thomas. We thank Dr. Robert Burghardt, Director of the Image Analysis Laboratory (College of Veterinary Medicine and Biomedical Sciences, Texas A&M University) for assistance in using the imaging facility. The Image Analysis Laboratory has been supported in part by National Institutes of Health Grants S10RR022532, P42ES004917, and P30ES009106.

REFERENCES

1. Bartel, D. P. (2009) *Cell* **136,** 215–233
2. Banerjee, D., Kwok, A., Lin, S. Y., and Slack, F. J. (2005) *Dev. Cell* **8,** 287–295
3. Cheng, H. Y., and Obrietan, K. (2007) *Cell Cycle* **6,** 3034–3035
4. O'Neill, J. S., and Hastings, M. H. (2007) *Curr. Biol.* **17,** R760–762
5. Xu, S., Witmer, P. D., Lumayag, S., Kovacs, B., and Valle, D. (2007) *J. Biol. Chem.* **282,** 25053–25066
6. Cheng, H. Y., Papp, J. W., Varlamova, O., Dziema, H., Russell, B., Curfman, J. P., Nakazawa, T., Shimizu, K., Okamura, H., Impey, S., and Obrietan, K. (2007) *Neuron* **54,** 813–829
7. Karali, M., Peluso, I., Marigo, V., and Banfi, S. (2007) *Invest. Ophthalmol. Vis. Sci.* **48,** 509–515
8. Ryan, D. G., Oliveira-Fernandes, M., and Lavker, R. M. (2006) *Mol. Vis.* **12,** 1175–1184
9. Boden, G., Ruiz, J., Urbain, J. L., and Chen, X. (1996) *Am. J. Physiol.* **271,** E246–E252
10. Bray, M. S., Shaw, C. A., Moore, M. W., Garcia, R. A., Zanquetta, M. M., Durgan, D. J., Jeong, W. J., Tsai, J. Y., Bugger, H., Zhang, D., Rohrwasser, A., Rennison, J. H., Dyck, J. R., Litwin, S. E., Hardin, P. E., Chow, C. W., Chandler, M. P., Abel, E. D., and Young, M. E. (2008) *Am. J. Physiol. Heart Circ. Physiol.* **294,** H1036–H1047
11. Dijk, D. J., and von Schantz, M. (2005) *J. Biol. Rhythms* **20,** 279–290
12. Fuller, P. M., Lu, J., and Saper, C. B. (2008) *Science* **320,** 1074–1077
13. Green, C. B., and Besharse, J. C. (2004) *J. Biol. Rhythms* **19,** 91–102
14. Cahill, G. M., and Besharse, J. C. (1993) *Neuron* **10,** 573–577
15. Pierce, M. E., Sheshberadaran, H., Zhang, Z., Fox, L. E., Applebury, M. L., and Takahashi, J. S. (1993) *Neuron* **10,** 579–584
16. Ivanova, T. N., and Iuvone, P. M. (2003) *Brain Res.* **991,** 96–103
17. Ivanova, T. N., and Iuvone, P. M. (2003) *Brain Res.* **973,** 56–63
18. Ko, G. Y., Ko, M. L., and Dryer, S. E. (2001) *Neuron* **29,** 255–266
19. Ko, M. L., Liu, Y., Dryer, S. E., and Ko, G. Y. (2007) *J. Neurochem.* **103,** 784–792
20. Remé, C., Wirz-Justice, A., Rhyner, A., and Hofmann, S. (1986) *Brain. Res.* **369,** 356–360
21. Spiwoks-Becker, I., Glas, M., Lasarzik, I., and Vollrath, L. (2004) *Eur. J. Neurosci* **19,** 1559–1571
22. Witkovsky, P. (2004) *Doc. Ophthalmol* **108,** 17–40
23. Bailey, M. J., Beremand, P. D., Hammer, R., Reidel, E., Thomas, T. L., and Cassone, V. M. (2004) *J. Biol. Chem.* **279,** 52247–52254
24. Ko, G. Y., Ko, M. L., and Dryer, S. E. (2003) *J. Neurosci.* **23,** 3145–3153
25. Ko, G. Y., Ko, M. L., and Dryer, S. E. (2004) *J. Neurosci.* **24,** 1296–1304
26. Ko, M. L., Jian, K., Shi, L., and Ko, G. Y. (2009) *J. Neurochem.* **108,** 1607–1620
27. Bodi, I., Mikala, G., Koch, S. E., Akhter, S. A., and Schwartz, A. (2005) *J. Clin. Invest.* **115,** 3306–3317
28. Barnes, S., and Kelly, M. E. (2002) *Adv. Exp. Med. Biol.* **514,** 465–476
29. Morgans, C. W., Bayley, P. R., Oesch, N. W., Ren, G., Akileswaran, L., and Taylor, W. R. (2005) *Vis. Neurosci.* **22,** 561–568
30. Zhou, H., Yu, K., McCoy, K. L., and Lee, A. (2005) *J. Biol. Chem.* **280,** 29612–29619
31. Sambrook, J., and Russell, D. (2001) *Molecular Cloning: A Laboratory Manual*, 3rd Ed., pp. 6.4–6.12, Cold Spring Harbor Laboratory, Cold Spring Harbor, NY
32. Shi, L., Jian, K., Ko, M. L., Trump, D., and Ko, G. Y. (2009) *J. Biol. Chem.* **284,** 3966–3975

33. Berger, E. M., Dubrovsky, E. B., Appleby, L., and Dubrovskaya, V. (2005) *In Vitro Cell Dev. Biol. Anim.* **41,** 12–18
34. Tohse, N., Mészáros, J., and Sperelakis, N. (1992) *Circ. Res.* **71,** 376–384
35. Bengert, P., and Dandekar, T. (2005) *Brief Bioinform.* **6,** 72–85
36. Zhao, Y., Samal, E., and Srivastava, D. (2005) *Nature* **436,** 214–220
37. Huang, K. M., Dentchev, T., and Stambolian, D. (2008) *Mamm. Genome* **19,** 510–516
38. Shen, J., Yang, X., Xie, B., Chen, Y., Swaim, M., Hackett, S. F., and Campochiaro, P. A. (2008) *Mol. Ther.* **16,** 1208–1216
39. Xu, S. (2009) *Prog. Retin. Eye Res.* **28,** 87–116
40. Altamirano, J., and Bers, D. M. (2007) *Circ. Res.* **101,** 590–597
41. Chong, N. W., Chaurasia, S. S., Haque, R., Klein, D. C., and Iuvone, P. M. (2003) *J. Neurochem.* **85,** 851–860
42. Lee, R. C., Feinbaum, R. L., and Ambros, V. (1993) *Cell* **75,** 843–854
43. Ruvkun, G. (2008) *Nat. Med.* **14,** 1041–1045
44. Bernard, M., Iuvone, P. M., Cassone, V. M., Roseboom, P. H., Coon, S. L., and Klein, D. C. (1997) *J. Neurochem.* **68,** 213–224
45. Chong, N. W., Bernard, M., and Klein, D. C. (2000) *J. Biol. Chem.* **275,** 32991–32998
46. Eide, E. J., Kang, H., Crapo, S., Gallego, M., and Virshup, D. M. (2005) *Methods Enzymol.* **393,** 408–418
47. Fukuhara, C., Liu, C., Ivanova, T. N., Chan, G. C., Storm, D. R., Iuvone, P. M., and Tosini, G. (2004) *J. Neurosci.* **24,** 1803–1811
48. Iuvone, P. M., Tosini, G., Pozdeyev, N., Haque, R., Klein, D. C., and Chaurasia, S. S. (2005) *Prog. Retin. Eye Res.* **24,** 433–456
49. Mao, D., Warner, E. A., Gurwitch, S. A., and Dowd, D. R. (1998) *Mol. Endocrinol.* **12,** 492–503
50. Obrietan, K., Impey, S., Smith, D., Athos, J., and Storm, D. R. (1999) *J. Biol. Chem.* **274,** 17748–17756
51. Shigeyoshi, Y., Taguchi, K., Yamamoto, S., Takekida, S., Yan, L., Tei, H., Moriya, T., Shibata, S., Loros, J. J., Dunlap, J. C., and Okamura, H. (1997) *Cell* **91,** 1043–1053
52. Kaupp, U. B., and Seifert, R. (2002) *Physiol. Rev.* **82,** 769–824
53. Chae, K. S., Ko, G. Y., and Dryer, S. E. (2007) *Invest. Ophthalmol. Vis. Sci.* **48,** 901–906
54. Morgans, C. W. (2001) *Invest. Ophthalmol. Vis. Sci.* **42,** 2414–2418
55. Aguda, B. D., Kim, Y., Piper-Hunter, M. G., Friedman, A., and Marsh, C. B. (2008) *Proc. Natl. Acad. Sci. U.S.A.* **105,** 19678–19683
56. Brennecke, J., Hipfner, D. R., Stark, A., Russell, R. B., and Cohen, S. M. (2003) *Cell* **113,** 25–36
57. Kuss, A. W., and Chen, W. (2008) *Curr. Neurol. Neurosci. Rep.* **8,** 190–197
58. Ronshaugen, M., Biemar, F., Piel, J., Levine, M., and Lai, E. C. (2005) *Genes Dev.* **19,** 2947–2952
59. Kapsimali, M., Kloosterman, W. P., de Bruijn, E., Rosa, F., Plasterk, R. H., and Wilson, S. W. (2007) *Genome Biol.* **8,** R173
60. Wong, C. F., and Tellam, R. L. (2008) *J. Biol. Chem.* **283,** 9836–9843
61. Luzi, E., Marini, F., Sala, S. C., Tognarini, I., Galli, G., and Brandi, M. L. (2008) *J. Bone Miner. Res.* **23,** 287–295
62. Du, K., and Montminy, M. (1998) *J. Biol. Chem.* **273,** 32377–32379
63. Baler, R., Covington, S., and Klein, D. C. (1997) *J. Biol. Chem.* **272,** 6979–6985
64. Travnickova-Bendova, Z., Cermakian, N., Reppert, S. M., and Sassone-Corsi, P. (2002) *Proc. Natl. Acad. Sci. U.S.A.* **99,** 7728–7733
65. Preitner, N., Damiola, F., Lopez-Molina, L., Zakany, J., Duboule, D., Albrecht, U., and Schibler, U. (2002) *Cell* **110,** 251–260
66. Shearman, L. P., Sriram, S., Weaver, D. R., Maywood, E. S., Chaves, I., Zheng, B., Kume, K., Lee, C. C., van der Horst, G. T., Hastings, M. H., and Reppert, S. M. (2000) *Science* **288,** 1013–1019
67. Hirayama, J., Sahar, S., Grimaldi, B., Tamaru, T., Takamatsu, K., Nakahata, Y., and Sassone-Corsi, P. (2007) *Nature* **450,** 1086–1090
68. Jakubcakova, V., Oster, H., Tamanini, F., Cadenas, C., Leitges, M., van der Horst, G. T., and Eichele, G. (2007) *Neuron* **54,** 831–843
69. Kim, W. Y., Geng, R., and Somers, D. E. (2003) *Proc. Natl. Acad. Sci. U.S.A.* **100,** 4933–4938